

# Nonperturbative renormalization of the chiral nucleon-nucleon interaction up to next-to-next-to-leading order

E. Marji,<sup>1,2</sup> A. Canul,<sup>1</sup> Q. MacPherson,<sup>1</sup> R. Winzer,<sup>1</sup> Ch. Zeoli,<sup>1,3</sup> D. R. Entem,<sup>4,\*</sup> and R. Machleidt<sup>1,†</sup>

<sup>1</sup>*Department of Physics, University of Idaho, Moscow, Idaho 83844, USA*

<sup>2</sup>*College of Western Idaho, Nampa, Idaho 83653, USA*

<sup>3</sup>*Department of Physics, Florida State University, Tallahassee, Florida 32306, USA*

<sup>4</sup>*Grupo de Física Nuclear, IUFFyM, Universidad de Salamanca, E-37008 Salamanca, Spain*

(Dated: July 1, 2021)

We study the nonperturbative renormalization of the nucleon-nucleon ( $NN$ ) interaction at next-to-leading order (NLO) and next-to-next-to-leading order (NNLO) of chiral effective field theory. A systematic variation of the cutoff parameter is performed for values below the chiral symmetry breaking scale of about 1 GeV. The accuracy of the predictions is determined by calculating the  $\chi^2$  for the reproduction of the  $NN$  data for energy intervals below pion-production threshold. At NLO,  $NN$  data are described well up to about 100 MeV laboratory energy and, at NNLO, up to about 200 MeV—with, essentially, cutoff independence for cutoffs between about 450 and 850 MeV.

PACS numbers: 13.75.Cs, 21.30.-x, 12.39.Fe, 11.10.Gh

Keywords: nucleon-nucleon interaction, chiral effective field theory, renormalization

## I. INTRODUCTION

During the past three decades, it has been demonstrated that chiral effective field theory (chiral EFT) represents a powerful tool to deal with hadronic interactions at low energy in a systematic and model-independent way (see Refs. [1, 2] for recent reviews). The systematics is provided by a low-energy expansion arranged in terms of the soft scale over the hard scale,  $(Q/\Lambda_\chi)^\nu$ , where  $Q$  is generic for an external momentum (nucleon three-momentum or pion four-momentum) or a pion mass and  $\Lambda_\chi \approx 1$  GeV the chiral symmetry breaking scale.

The early applications of chiral perturbation theory (ChPT) focused on systems like  $\pi\pi$  [3] and  $\pi N$  [4], where the Goldstone-boson character of the pion guarantees that a perturbative expansion exists. But the past 20 years have also seen great progress in applying ChPT to nuclear forces [1, 2, 5–12]. The nucleon-nucleon ( $NN$ ) system is characterized by large scattering lengths and bound states indicating the nonperturbative character of the problem. Weinberg [5] therefore suggested to calculate the nuclear amplitude in two steps. In step one, the *nuclear potential*,  $\widehat{V}$ , is defined as the sum of irreducible diagrams, which are evaluated *perturbatively* up to the given order. Then in step two, this potential is iterated to all order (i.e., summed up *nonperturbatively*) in the Schrödinger or Lippmann-Schwinger (LS) equation:

$$\begin{aligned} \widehat{T}(\vec{p}', \vec{p}) &= \widehat{V}(\vec{p}', \vec{p}) + \int d^3p'' \widehat{V}(\vec{p}', \vec{p}'') \\ &\quad \times \frac{M_N}{p^2 - p''^2 + i\epsilon} \widehat{T}(\vec{p}'', \vec{p}), \end{aligned} \quad (1)$$

where  $\widehat{T}$  denotes the  $NN$  T-matrix and  $M_N$  the nucleon mass.

In general, the integral in the LS equation is divergent and needs to be regularized. Therefore, the potential  $\widehat{V}$  is multiplied with the regulator function  $f(p', p)$ ,

$$\widehat{V}(\vec{p}', \vec{p}) \mapsto \widehat{V}(\vec{p}', \vec{p}) f(p', p) \quad (2)$$

with

$$f(p', p) = \exp[-(p'/\Lambda)^{2n} - (p/\Lambda)^{2n}]. \quad (3)$$

Typical choices for the cutoff parameter  $\Lambda$  that appears in the regulator are  $\Lambda \approx 0.5$  GeV  $<$   $\Lambda_\chi \approx 1$  GeV.

It is pretty obvious that results for the T-matrix may depend sensitively on the regulator and its cutoff parameter. This is acceptable if one wishes to build models. For example, the meson models of the past [13] always depended sensitively on the choices for the cutoffs which, in fact, were used as additional fit parameters (besides the coupling constants). However, the EFT approach is expected to be model-independent.

In field theories, divergent integrals are not uncommon and methods have been developed for how to deal with them. One regulates the integrals and then removes the dependence on the regularization parameters (scales, cutoffs) by renormalization. In the end, the theory and its predictions do not depend on cutoffs or renormalization scales. So-called renormalizable quantum field theories, like QED, have essentially one set of prescriptions that takes care of renormalization through all orders. In contrast, EFTs are renormalized order by order.

Weinberg's implicit assumption [5, 14] was that the counterterms introduced to renormalize the perturbatively calculated potential, based upon naive dimensional analysis (“Weinberg counting”), are also sufficient to renormalize the nonperturbative resummation of the potential in the LS equation. In 1996, Kaplan, Savage, and Wise (KSW) [15] pointed out that there are problems

\*Electronic address: entem@usal.es

†Electronic address: machleidt@uidaho.edu

with the Weinberg scheme if the LS equation is renormalized by minimally-subtracted dimensional regularization. This criticism resulted in a flurry of publications on the renormalization of the nonperturbative  $NN$  problem. The literature is too comprehensive to elaborate on all contributions. Therefore, we will restrict ourselves, here, to discussing just a few aspects that we perceive as particularly important. A more comprehensive consideration can be found in Ref. [1]

Naively, the ideal renormalization procedure is the one where the cutoff parameter  $\Lambda$  is carried to infinity while stable results are maintained. This was done successfully at leading order (LO) in the work by Nogga *et al* [16]. At next-to-next-to-leading order (NNLO), the infinite-cutoff renormalization procedure has been investigated in [17] for partial waves with total angular momentum  $J \leq 1$  and in [18] for all partial waves with  $J \leq 5$ . At next-to-next-to-next-to-leading order (N<sup>3</sup>LO), the  $^1S_0$  state was considered in Ref. [19], and all states up to  $J = 6$  were investigated in Ref. [20]. From all of these works, it is evident that no counter term is effective in partial-waves with short-range repulsion and only a single counter term can effectively be used in partial-waves with short-range attraction. Thus, for the  $\Lambda \rightarrow \infty$  renormalization prescription, even at N<sup>3</sup>LO, there exists either one or no counter term per partial-wave state. This is inconsistent with any reasonable power-counting scheme and prevents an order-by-order improvement of the predictions.

To summarize: In the infinite-cutoff renormalization scheme, the potential is applied up to unlimited momenta. However, the EFT this potential is derived from has validity only for momenta smaller than the chiral symmetry breaking scale  $\Lambda_\chi \approx 1$  GeV. The lack of order-by-order convergence and discrepancies in lower partial-waves demonstrate that the potential should not be used beyond the limits of the effective theory [20] (see Ref. [21] for a related discussion). The conclusion then is that cutoffs should be limited to  $\Lambda \lesssim \Lambda_\chi$  (but see also Ref. [22]).

A possible solution of this problem was proposed already in [16] and reiterated in a paper by Long and van Kolck [23]. A calculation of the proposed kind has been performed by Valderrama [24], for the  $S$ ,  $P$ , and  $D$  waves. The author renormalizes the LO interaction nonperturbatively and then uses the LO distorted wave to calculate the two-pion-exchange contributions at NLO and NNLO perturbatively. It turns out that perturbative renormalizability requires the introduction of about twice as many counter terms as compared to Weinberg counting, which reduces the predictive power. The order-by-order convergence of the  $NN$  phase shifts appears to be reasonable, but the cutoffs used in this perturbative summations are rather soft.

However, even if one considers the above method as successful for  $NN$  scattering, there is doubt if the interaction generated in this approach is of any use for applications in nuclear few- and many-body problems. In these applications, one would first have to solve the many-body problem with the re-summed LO interaction, and then

add higher order corrections in perturbation theory. It was shown in a recent paper [25] that the renormalized LO interaction is characterized by a very large tensor force from one-pion-exchange (1PE). This is no surprise since LO is renormalized with  $\Lambda \rightarrow \infty$  implying that the 1PE, particularly its tensor force, is totally uncut. As a consequence of this, the wound integral in nuclear matter,  $\kappa$ , comes out to be about 40%. The hole-line and coupled cluster expansions are known to converge  $\propto \kappa^{n-1}$  with  $n$  the number of hole-lines or particles per cluster. For conventional nuclear forces, the wound integral is typically between 5 and 10% and the inclusion of three-body clusters (or three hole-lines) are needed to obtain converged results in the many-body system. Thus, if the wound integral is 40%, probably, up to six hole-lines need to be included for approximate convergence. Such calculations are not feasible even with the most powerful computers of today and will not be feasible any time soon. Therefore, even if the renormalization procedure proposed in [23] will work for  $NN$  scattering, the interaction produced will be highly impractical (to say the least) in applications in few- and many-body systems because of convergence problems with the many-body energy and wave functions.

The various problems with the renormalization procedures discussed above may have a simple common reason: An EFT that has validity only for momenta  $Q < \Lambda_\chi$  is applied such that momenta  $Q \gg \Lambda_\chi$  are heavily involved (because the regulator cutoff parameter  $\Lambda$  is taken to infinity). A recent paper by Epelbaum and Gegelia [21] illustrates the point: The authors construct an exactly solvable toy-model that simulates a pionful EFT and yields finite results for  $\Lambda \rightarrow \infty$ . However, as it turns out, these finite results are incompatible with the underlying EFT, while for cutoffs in the order of the hard scale consistency is maintained. In simple terms, the point to realize is this: If an EFT calculation produces (accidentally) a finite result for  $\Lambda \rightarrow \infty$ , then that does not automatically imply that this result is also meaningful.

This matter is further elucidated in the lectures by Lepage of 1997 [26]. Lepage points out that it makes little sense to take the momentum cutoff beyond the range of validity of the effective theory. By assumption, our data involves energies that are too low—wave lengths that are too long—to probe the true structure of the theory at very short distances. When one goes beyond the hard-scale of the theory, structures are seen that are almost certainly wrong. Thus, results cannot improve and, in fact, they may degrade or, in more extreme cases, the theory may become unstable or untunable. In fact, in the  $NN$  case, this is what is happening in several partial waves (as reported above). Therefore, Lepage suggests to take the following three steps when building an effective theory:

1. Incorporate the correct long-range behavior: The long-range behavior of the underlying theory must be known, and it must be built into the effective theory. In the case of nuclear forces, the long-range

theory is, of course, well known and given by one- and multi-pion exchanges.

2. Introduce an ultraviolet cutoff to exclude high-momentum states, or, equivalent, to soften the short-distance behavior: The cutoff has two effects: First it excludes high-momentum states, which are sensitive to the unknown short-distance dynamics; only states that we understand are retained. Second it makes all interactions regular at  $r = 0$ , thereby avoiding infinities.
3. Add local correction terms (also known as contact or counter terms) to the effective Hamiltonian. These mimic the effects of the high-momentum states excluded by the cutoff introduced in the previous step. In the meson-exchange picture, the short-range nuclear force is described by heavy meson exchange, like the  $\rho(770)$  and  $\omega(782)$ . However, at low energy, such structures are not resolved. Since we must include contact terms anyhow, it is most efficient to use them to account for any heavy-meson exchange as well. The correction terms systematically remove dependence on the cutoff.

Crucial for an EFT are regulator independence (within the range of validity of the EFT) and a power counting scheme that allows for order-by-order improvement with decreasing truncation error. The purpose of renormalization is to achieve this regulator independence while maintaining a functional power counting scheme.

Thus, in the spirit of Lepage [26], the cutoff independence should be examined for cutoffs below the hard scale and not beyond. Ranges of cutoff independence within the theoretical error are to be identified. In this paper, we will present a systematic investigation of this kind. In our work, we quantify the error of the predictions by calculating the  $\chi^2/\text{datum}$  for the reproduction of the neutron-proton ( $np$ ) elastic scattering data as a function of the cutoff parameter  $\Lambda$  of the regulator Eq. (3). We will investigate the predictions by chiral  $np$  potentials at order NLO and NNLO applying Weinberg counting for the counter terms ( $NN$  contact terms).

This paper is organized as follows. In Sec. II, we present the mathematical formalism which defines chiral  $NN$  potentials up to NNLO and  $NN$  scattering. In Sec. III, we discuss in detail the nonperturbative renormalization of these potentials and present our results. The paper is concluded in Sec. IV.

## II. CHIRAL $NN$ POTENTIAL AND TWO-NUCLEON SCATTERING

Nuclear potentials are defined as sets of irreducible graphs up to a given order. The power  $\nu$  of a few-nucleon diagram involving  $A$  nucleons is given in terms of naive

dimensional analysis by:

$$\nu = -2 + 2A - 2C + 2L + \sum_i \Delta_i, \quad (4)$$

with

$$\Delta_i \equiv d_i + \frac{n_i}{2} - 2, \quad (5)$$

where  $C$  denotes the number of separately connected pieces and  $L$  the number of loops in the diagram;  $d_i$  is the number of derivatives or pion-mass insertions and  $n_i$  the number of nucleon fields (nucleon legs) involved in vertex  $i$ ; the sum runs over all vertices contained in the diagram under consideration. Note that  $\Delta_i \geq 0$  for all interactions allowed by chiral symmetry. For an irreducible  $NN$  diagram (“two-nucleon potential”,  $A = 2$ ,  $C = 1$ ), Eq. (4) collapses to

$$\nu = 2L + \sum_i \Delta_i. \quad (6)$$

Thus, in terms of naive dimensional analysis or “Weinberg counting”, the various orders of the irreducible graphs which define the chiral  $NN$  potential are given by:

$$V_{\text{LO}} = V_{\text{ct}}^{(0)} + V_{1\pi}^{(0)} \quad (7)$$

$$V_{\text{NLO}} = V_{\text{LO}} + V_{\text{ct}}^{(2)} + V_{1\pi}^{(2)} + V_{2\pi}^{(2)} \quad (8)$$

$$V_{\text{NNLO}} = V_{\text{NLO}} + V_{1\pi}^{(3)} + V_{2\pi}^{(3)} \quad (9)$$

where the superscript denotes the order  $\nu$  of the low-momentum expansion. Contact potentials carry the subscript “ct” and pion-exchange potentials can be identified by an obvious subscript.

The charge-independent 1PE potential reads

$$V_{1\pi}(\vec{p}', \vec{p}) = -\frac{g_A^2}{4f_\pi^2} \boldsymbol{\tau}_1 \cdot \boldsymbol{\tau}_2 \frac{\vec{\sigma}_1 \cdot \vec{q} \vec{\sigma}_2 \cdot \vec{q}}{q^2 + m_\pi^2}, \quad (10)$$

where  $\vec{p}'$  and  $\vec{p}$  designate the final and initial nucleon momenta in the center-of-mass system (CMS) and  $\vec{q} \equiv \vec{p}' - \vec{p}$  is the momentum transfer;  $\vec{\sigma}_{1,2}$  and  $\boldsymbol{\tau}_{1,2}$  are the spin and isospin operators of nucleon 1 and 2;  $g_A$ ,  $f_\pi$ , and  $m_\pi$  denote axial-vector coupling constant, the pion decay constant, and the pion mass, respectively. We use  $f_\pi = 92.4$  MeV and  $g_A = 1.29$  throughout this work. Since higher order corrections contribute only to mass and coupling constant renormalizations and since, on shell, there are no relativistic corrections, the on-shell 1PE has the form Eq. (10) in all orders.

In this paper, we will specifically calculate neutron-proton ( $np$ ) scattering and take the charge-dependence (isospin violation) of the 1PE into account. Thus, the 1PE potential that we actually apply reads

$$V_{1\pi}^{(np)}(\vec{p}', \vec{p}) = -V_{1\pi}(m_{\pi^0}) + (-1)^{I+1} 2 V_{1\pi}(m_{\pi^\pm}), \quad (11)$$

where  $I$  denotes the isospin of the two-nucleon system and

$$V_{1\pi}(m_\pi) \equiv -\frac{g_A^2}{4f_\pi^2} \frac{\vec{\sigma}_1 \cdot \vec{q} \vec{\sigma}_2 \cdot \vec{q}}{q^2 + m_\pi^2}. \quad (12)$$

We use  $m_{\pi^0} = 134.9766$  MeV and  $m_{\pi^\pm} = 139.5702$  MeV.

### A. Leading order (LO)

The LO chiral  $NN$  potential consists of a contact part and an 1PE part, cf. Eq. (7). The 1PE part is given by Eq. (11) and the LO contacts are

$$V_{\text{ct}}^{(0)}(\vec{p}', \vec{p}) = C_S + C_T \vec{\sigma}_1 \cdot \vec{\sigma}_2, \quad (13)$$

and, in terms of partial waves,

$$\begin{aligned} V_{\text{ct}}^{(0)}(^1S_0) &= \tilde{C}_{1S_0} = 4\pi(C_S - 3C_T) \\ V_{\text{ct}}^{(0)}(^3S_1) &= \tilde{C}_{3S_1} = 4\pi(C_S + C_T), \end{aligned} \quad (14)$$

where  $C_S, C_T, \tilde{C}_{1S_0}, \tilde{C}_{3S_1}$  are constants to be adjusted to  $NN$  data.

### B. Next-to-leading order (NLO)

For the NLO chiral  $NN$  potential, Eq. (8), we need to specify the second order contact part and the two-pion exchange (2PE) part. The NLO contact terms are given by [1]

$$\begin{aligned} V_{\text{ct}}^{(2)}(\vec{p}', \vec{p}) &= C_1 q^2 + C_2 k^2 \\ &+ (C_3 q^2 + C_4 k^2) \vec{\sigma}_1 \cdot \vec{\sigma}_2 \\ &+ C_5 \left( -i\vec{S} \cdot (\vec{q} \times \vec{k}) \right) \\ &+ C_6 (\vec{\sigma}_1 \cdot \vec{q}) (\vec{\sigma}_2 \cdot \vec{q}) \\ &+ C_7 (\vec{\sigma}_1 \cdot \vec{k}) (\vec{\sigma}_2 \cdot \vec{k}), \end{aligned} \quad (15)$$

with the partial-wave decomposition

$$\begin{aligned} V_{\text{ct}}^{(2)}(^1S_0) &= C_{1S_0}(p^2 + p'^2) \\ V_{\text{ct}}^{(2)}(^3P_0) &= C_{3P_0} pp' \\ V_{\text{ct}}^{(2)}(^1P_1) &= C_{1P_1} pp' \\ V_{\text{ct}}^{(2)}(^3P_1) &= C_{3P_1} pp' \\ V_{\text{ct}}^{(2)}(^3S_1) &= C_{3S_1}(p^2 + p'^2) \\ V_{\text{ct}}^{(2)}(^3S_1 - ^3D_1) &= C_{3S_1 - ^3D_1} p^2 \\ V_{\text{ct}}^{(2)}(^3D_1 - ^3S_1) &= C_{3S_1 - ^3D_1} p'^2 \\ V_{\text{ct}}^{(2)}(^3P_2) &= C_{3P_2} pp'. \end{aligned} \quad (16)$$

To state the 2PE potentials, we introduce the following scheme:

$$\begin{aligned} V_{2\pi}^{(\nu)}(\vec{p}', \vec{p}) &= V_C^{(\nu)} + \tau_1 \cdot \tau_2 W_C^{(\nu)} \\ &+ \left[ V_S^{(\nu)} + \tau_1 \cdot \tau_2 W_S^{(\nu)} \right] \vec{\sigma}_1 \cdot \vec{\sigma}_2 \\ &+ \left[ V_{LS}^{(\nu)} + \tau_1 \cdot \tau_2 W_{LS}^{(\nu)} \right] \left( -i\vec{S} \cdot (\vec{q} \times \vec{k}) \right) \\ &+ \left[ V_T^{(\nu)} + \tau_1 \cdot \tau_2 W_T^{(\nu)} \right] \vec{\sigma}_1 \cdot \vec{q} \vec{\sigma}_2 \cdot \vec{q} \\ &+ \left[ V_{\sigma L}^{(\nu)} + \tau_1 \cdot \tau_2 W_{\sigma L}^{(\nu)} \right] \vec{\sigma}_1 \cdot (\vec{q} \times \vec{k}) \vec{\sigma}_2 \cdot (\vec{q} \times \vec{k}), \end{aligned} \quad (17)$$

where

$$\begin{aligned} \vec{k} &\equiv \frac{1}{2}(\vec{p}' + \vec{p}) \quad \text{is the average momentum, and} \\ \vec{S} &\equiv \frac{1}{2}(\vec{\sigma}_1 + \vec{\sigma}_2) \quad \text{the total spin.} \end{aligned} \quad (18)$$

Using the above notation, the NLO 2PE is simply given by [1, 7]

$$\begin{aligned} W_C^{(2)} &= -\frac{L(q)}{384\pi^2 f_\pi^4} \left[ 4m_\pi^2(5g_A^4 - 4g_A^2 - 1) \right. \\ &\quad \left. + q^2(23g_A^4 - 10g_A^2 - 1) + \frac{48g_A^4 m_\pi^4}{w^2} \right], \end{aligned} \quad (19)$$

$$V_T^{(2)} = -\frac{1}{q^2} V_S^{(2)} = -\frac{3g_A^4 L(q)}{64\pi^2 f_\pi^4}. \quad (20)$$

It is well known that the 2PE at NNLO shows an unphysically strong attraction in the high-momentum components of the loop integrals, when regularized by dimensional regularization. For a realistic 2PE contribution at order NNLO, it is therefore necessary to cut out those short-range components. This can be achieved by applying the so-called spectral function regularization (SFR) in those loop integrals (see Ref. [27] for details), which leads to the following loop function:

$$L(q) \equiv \theta(\tilde{\Lambda} - 2m_\pi) \frac{w}{2q} \ln \frac{\tilde{\Lambda}^2 w^2 + q^2 s^2 + 2\tilde{\Lambda} q w s}{4m_\pi^2 (\tilde{\Lambda}^2 + q^2)} \quad (21)$$

with

$$w \equiv \sqrt{4m_\pi^2 + q^2} \quad \text{and} \quad (22)$$

$$s \equiv \sqrt{\tilde{\Lambda}^2 - 4m_\pi^2}. \quad (23)$$

Note that

$$\lim_{\tilde{\Lambda} \rightarrow \infty} L(q) = \frac{w}{q} \ln \frac{w+q}{2m_\pi}, \quad (24)$$

which is the loop function used in dimensional regularization. SFR introduces the cutoff parameter  $\tilde{\Lambda}$ , for which a value below the chiral-symmetry breaking scale of  $\sim 1$  GeV is appropriate. For our choices for  $\tilde{\Lambda}$ , see below. SFR is not really necessary for the NLO contribution, but since we have to use it for NNLO, we apply this also at NLO for reasons of consistency.

### C. Next-to-next-to-leading order (NNLO)

There are no new contacts at NNLO, cf. Eq. (9), and, thus, all we need is the third order 2PE potential, which is [using the notation introduced in Eq. (17)] [1, 7]

$$V_C^{(3)} = V_{C1}^{(3)} + V_{C2}^{(3)}, \quad (25)$$

$$W_C^{(3)} = W_{C1}^{(3)} + W_{C2}^{(3)}, \quad (26)$$

$$V_T^{(3)} = V_{T1}^{(3)} + V_{T2}^{(3)}, \quad (27)$$

$$W_T^{(3)} = W_{T1}^{(3)} + W_{T2}^{(3)}, \quad (28)$$

$$V_S^{(3)} = V_{S1}^{(3)} + V_{S2}^{(3)}, \quad (29)$$

$$W_S^{(3)} = W_{S1}^{(3)} + W_{S2}^{(3)}, \quad (30)$$

$$V_{LS}^{(3)} = \frac{3g_A^4 \tilde{w}^2 A(q)}{32\pi M_N f_\pi^4}, \quad (31)$$

$$W_{LS}^{(3)} = \frac{g_A^2 (1 - g_A^2)}{32\pi M_N f_\pi^4} w^2 A(q), \quad (32)$$

where

$$V_{C1}^{(3)} = \frac{3g_A^2}{16\pi f_\pi^4} \left\{ \frac{g_A^2 m_\pi^5}{16M_N w^2} - \left[ 2m_\pi^2 (2c_1 - c_3) - q^2 \left( c_3 + \frac{3g_A^2}{16M_N} \right) \right] \tilde{w}^2 A(q) \right\}, \quad (33)$$

$$W_{C1}^{(3)} = \frac{g_A^2}{128\pi M_N f_\pi^4} \left\{ 3g_A^2 m_\pi^5 w^{-2} - [4m_\pi^2 + 2q^2 - g_A^2 (4m_\pi^2 + 3q^2)] \tilde{w}^2 A(q) \right\}, \quad (34)$$

$$V_{T1}^{(3)} = -\frac{1}{q^2} V_{S1}^{(3)} = \frac{9g_A^4 \tilde{w}^2 A(q)}{512\pi M_N f_\pi^4}, \quad (35)$$

$$W_{T1}^{(3)} = -\frac{1}{q^2} W_{S1}^{(3)} = -\frac{g_A^2 A(q)}{32\pi f_\pi^4} \times \left[ \left( c_4 + \frac{1}{4M_N} \right) w^2 - \frac{g_A^2}{8M_N} (10m_\pi^2 + 3q^2) \right], \quad (36)$$

and

$$V_{C2}^{(3)} = -\frac{3g_A^4}{256\pi f_\pi^4 M_N} (m_\pi w^2 + \tilde{w}^4 A(q)), \quad (37)$$

$$W_{C2}^{(3)} = \frac{g_A^4}{128\pi f_\pi^4 M_N} (m_\pi w^2 + \tilde{w}^4 A(q)), \quad (38)$$

$$V_{T2}^{(3)} = -\frac{1}{q^2} V_{S2}^{(3)} = \frac{3g_A^4}{512\pi f_\pi^4 M_N} (m_\pi + w^2 A(q)), \quad (39)$$

$$W_{T2}^{(3)} = -\frac{1}{q^2} W_{S2}^{(3)} = -\frac{g_A^4}{256\pi f_\pi^4 M_N} (m_\pi + w^2 A(q)), \quad (40)$$

with

$$\tilde{w} \equiv \sqrt{2m_\pi^2 + q^2}. \quad (41)$$

The loop function that appears in the above expressions, regularized by SFR, is

$$A(q) \equiv \theta(\tilde{\Lambda} - 2m_\pi) \frac{1}{2q} \arctan \frac{q(\tilde{\Lambda} - 2m_\pi)}{q^2 + 2\tilde{\Lambda}m_\pi}. \quad (42)$$

$$\lim_{\tilde{\Lambda} \rightarrow \infty} A(q) = \frac{1}{2q} \arctan \frac{q}{2m_\pi} \quad (43)$$

yields the loop function used in dimensional regularization. Note that Eqs. (37)-(40) are corrections of the iterative 2PE, see Ref. [1] for details. In all 2PE potentials, we apply the average nucleon mass,  $M_N = 938.9182$  MeV, and the average pion mass,  $m_\pi = 138.039$  MeV. For the dimension-two low-energy constants we use  $c_1 = -0.81$  GeV<sup>-1</sup>,  $c_3 = -3.40$  GeV<sup>-1</sup>, and  $c_4 = 3.40$  GeV<sup>-1</sup> [28].

### D. NN scattering

For the unitarizing scattering equation, we choose the relativistic three-dimensional equation proposed by Blankenbecler and Sugar (BbS) [29], which reads,

$$T(\vec{p}', \vec{p}) = V(\vec{p}', \vec{p}) + \int \frac{d^3 p''}{(2\pi)^3} V(\vec{p}', \vec{p}'') \times \frac{M_N^2}{E_{p''}} \frac{1}{p^2 - p''^2 + i\epsilon} T(\vec{p}'', \vec{p}) \quad (44)$$

with  $E_{p''} \equiv \sqrt{M_N^2 + p''^2}$ . The advantage of using a relativistic scattering equation is that it automatically includes relativistic corrections to all orders. Thus, in the scattering equation, no propagator modifications are necessary when raising the order to which the calculation is conducted.

Defining

$$\hat{V}(\vec{p}', \vec{p}) \equiv \frac{1}{(2\pi)^3} \sqrt{\frac{M_N}{E_{p'}}} V(\vec{p}', \vec{p}) \sqrt{\frac{M_N}{E_p}} \quad (45)$$

and

$$\hat{T}(\vec{p}', \vec{p}) \equiv \frac{1}{(2\pi)^3} \sqrt{\frac{M_N}{E_{p'}}} T(\vec{p}', \vec{p}) \sqrt{\frac{M_N}{E_p}}, \quad (46)$$

where the factor  $1/(2\pi)^3$  is added for convenience, the BbS equation collapses into the usual, nonrelativistic Lippmann-Schwinger (LS) equation, Eq. (1). Since  $\hat{V}$  satisfies Eq. (1), it can be used like a usual nonrelativistic potential, and  $\hat{T}$  may be perceived as the conventional nonrelativistic T-matrix. The square-root factors in Eqs. (45) and (46) are applied to the potentials of all orders.

In the LS equation, Eq. (1), we use

$$M_N = \frac{2M_p M_n}{M_p + M_n} = 938.9182 \text{ MeV}, \text{ and} \quad (47)$$

$$p^2 = \frac{M_p^2 T_{\text{lab}} (T_{\text{lab}} + 2M_n)}{(M_p + M_n)^2 + 2T_{\text{lab}} M_p}, \quad (48)$$

where  $M_p = 938.2720$  MeV and  $M_n = 939.5653$  MeV are the proton and neutron masses, respectively, and  $T_{\text{lab}}$  is the kinetic energy of the incident neutron in the laboratory system ("Lab. Energy"). The relationship between  $p^2$  and  $T_{\text{lab}}$  is based upon relativistic kinematics.

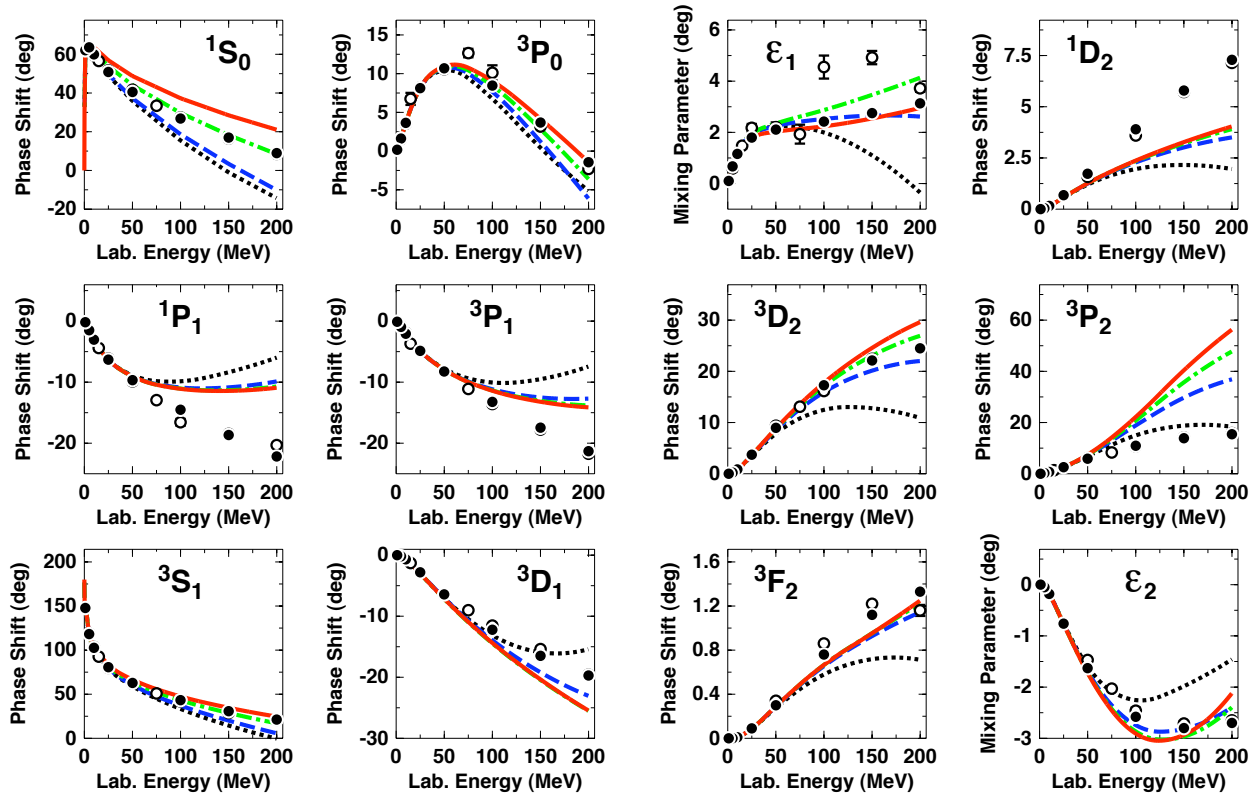


FIG. 1: (Color online). Phase-shifts of neutron-proton scattering at order NLO for total angular momentum  $J \leq 2$  and laboratory kinetic energies below 200 MeV. The black dotted curve is obtained for  $\Lambda = 400$  MeV, the blue dashed curve for  $\Lambda = 600$  MeV, the green dash-dot curve for  $\Lambda = 800$  MeV, and the red solid curve for  $\Lambda = 1000$  MeV. The value for the SFR parameter is  $\tilde{\Lambda} = 700$  MeV. The filled and open circles represent the results from the Nijmegen multi-energy  $np$  phase-shift analysis [31] and the VPI/GWU single-energy  $np$  analysis SM99 [32], respectively.

### III. NONPERTURBATIVE RENORMALIZATION

The chiral  $NN$  potential depends on two cutoff parameters,  $\tilde{\Lambda}$  and  $\Lambda$ . The parameter  $\tilde{\Lambda}$  is introduced for the SFR of the pion loop integrals. The SFR cuts out the short range part of the 2PE. To be more specific: Short distance contributions, which are equivalent to contributions from “meson masses”  $m > \tilde{\Lambda}$ , are set to zero. This is necessary, because the short-range part of the 2PE shows unphysically strong attraction, particularly, at NNLO. All this is part of the evaluation of the potential which is calculated and renormalized perturbatively. It has nothing to do with nonperturbative regularization and renormalization. The parameter  $\tilde{\Lambda}$  is given a fixed value in the order of the  $\rho$  mass or slightly below.

The process of interest in this paper is the re-summation of the potential in the LS equation (1), which is a nonperturbative process. To avoid divergences in the re-summation, the regulator Eq. (3) is applied, which is a function of the cutoff parameter  $\Lambda$ . The renormalization of this regularized LS equation is the focus of the present investigation. Successful renormalization means independence of the predictions from  $\Lambda$  within the accu-

racy of the given order. To investigate this issue, we vary  $\Lambda$  from about 350 MeV to 900 MeV.

We choose this range of cutoff values for the following reasons. Choosing  $\Lambda$  too small removes the long-distance physics in which we trust. We certainly want to preserve the chiral 2PE contribution to the  $NN$  interaction. Two pions have a rest-mass of about 280 MeV. In addition, the pions have kinetic energy. This suggests 350 MeV as a reasonable guess for a lower limit, but see discussion below. The upper limit for cutoffs is dictated by the fact that  $\Lambda$  should be below the chiral symmetry breaking scale  $\Lambda_\chi \sim 1$  GeV.

For each value of  $\Lambda$ , the  $S$ - and  $P$ -waves are readjusted with the help of the seven counter terms available at NLO and NNLO, cf. Eqs. (14) and (16).  $S$ -waves carry two counter terms each. In  $^1S_0$ , we use them to adjust the scattering length,  $a_s$ , and the effective range,  $r_s$ , to their empirical values,

$$a_s = -23.74 \text{ fm}, \quad (49)$$

$$r_s = 2.70 \text{ fm}. \quad (50)$$

While it is always possible to fit  $a_s$  accurately, there are problems fitting  $r_s$  for the higher values of  $\Lambda$ , in which case we fit  $r_s$  as close as possible.

In  $^3S_1$ , we fit the deuteron binding energy,  $B_d$ , and the effective range,  $r_t$ ,

$$B_d = 2.224575 \text{ MeV}, \quad (51)$$

$$r_t = 1.75 \text{ fm}. \quad (52)$$

Similar to the  $^1S_0$  case, the  $r_t$  cannot be fit accurately for the larger values of  $\Lambda$ , where we then fit  $r_t$  as close as possible.  $B_d$  is always reproduced accurately.

$P$ -waves have one counter term each, which we utilize to fit the empirical phase shifts at 25 MeV as determined in the Nijmegen multienergy  $np$  phase shift analysis [31], which are:

$$\delta_{1P_1}(25 \text{ MeV}) = -6.31 \text{ deg}, \quad (53)$$

$$\delta_{3P_0}(25 \text{ MeV}) = 8.13 \text{ deg}, \quad (54)$$

$$\delta_{3P_1}(25 \text{ MeV}) = -4.88 \text{ deg}, \quad (55)$$

$$\delta_{3P_1}(25 \text{ MeV}) = 2.56 \text{ deg}. \quad (56)$$

Finally, the contact parameter of the  $^3S_1 - ^3D_1$  transition potential,  $C_{3S_1-3D_1}$  [Eq. (16)], is adjusted such that the  $\epsilon_1$  mixing parameter at 25 MeV reproduces the Nijmegen value,

$$\epsilon_1(25 \text{ MeV}) = 1.79 \text{ deg}. \quad (57)$$

In previous studies, investigators looked at the  $NN$  phase shifts to judge if there was independence from the cutoff parameter within the presumed accuracy [9, 16, 17, 30]. However, from phase shifts it is difficult to extract the over-all error, because the deviations from the empirical phase shifts can be very different in different partial waves, see Fig 1. Moreover, it is well-known from the early days of phase-shift analysis that there may exist several different phase-shift solutions all of which fit the  $NN$  data about equally well. This is due to the fact that the deviation from a particular phase shift solution in one partial wave may be compensated by a deviation in some other partial wave. The only uniquely defined  $NN$  data are the original experimental data of  $NN$  observable measurements. Therefore, in the present investigation, we determine the accuracy of the predictions by calculating the  $\chi^2$  for the reproduction of the  $NN$  data:

$$\chi^2 = \sum_{i=1}^N \left( \frac{x_i^{\text{theo}} - x_i^{\text{exp}}}{\Delta x_i^{\text{exp}}} \right)^2, \quad (58)$$

where  $N$  denotes the total number of experimental data (including normalizations),  $x_i^{\text{theo}}$  is the prediction for datum  $i$ , and  $x_i^{\text{exp}}$  the experimental value with uncertainty  $\Delta x_i^{\text{exp}}$ . In general, we will state results for the  $\chi^2$  in terms of  $\chi^2/\text{datum} \equiv \chi^2/N$ .

To be more specific, we consider  $np$  scattering and thus compare to the  $np$  data. The  $np$  system has the advantage that it includes  $I = 0$  and  $I = 1$  and, thus, covers all  $NN$  partial waves. We consider energies up to pion-production threshold. Since the accuracy of the predictions by chiral EFT is energy dependent, we subdivide the total energy range below pion-production threshold into four intervals and calculate the  $\chi^2$  for those intervals. The intervals are shown in the  $\chi^2$  tables below.

TABLE I:  $\chi^2/\text{datum}$  for the reproduction of the  $np$  data at NLO for various values for  $\Lambda$  of the regulator function Eq. (3). Results are given for two choices for the SFR parameter, namely,  $\tilde{\Lambda} = 700 \text{ MeV}$  and  $\tilde{\Lambda} \rightarrow \infty$  (in parentheses).  $T_{\text{lab}}$  denotes the kinetic energy of the incident neutron in the laboratory system.

$T_{\text{lab}}$ bin (MeV)	$\Lambda$ (MeV)					
	400	500	600	700	800	900
2-35	1.12 (1.17)	1.03 (1.04)	1.03 (1.07)	1.21 (1.25)	2.11 (1.94)	3.33 (2.85)
35-125	11.1 (12.0)	6.12 (6.44)	4.79 (4.98)	3.98 (4.16)	4.77 (5.63)	6.93 (8.64)
125-183	69.7 (75.9)	74.3 (76.5)	86.2 (88.3)	103 (95.3)	102 (96.8)	108 (104)

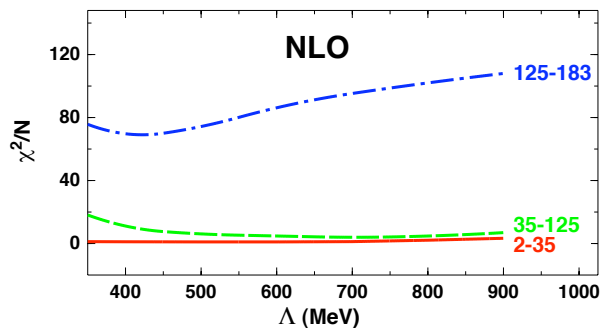


FIG. 2: (color online).  $\chi^2/\text{datum}$  for the reproduction of the  $np$  data at NLO as a function of the cutoff parameter  $\Lambda$  of the regulator Eq. (3). Results are shown for various energy intervals as denoted in units of MeV. The SFR parameter is always  $\tilde{\Lambda} = 700 \text{ MeV}$ .

### A. Renormalization at NLO

At NLO, we use  $n = 2$  in the regulator function Eq. (3) and vary  $\Lambda$  from 350 to 900 MeV. For reasons of efficiency, we calculate the  $\chi^2$  at this order with the help of the Nijmegen error matrix [33]. We have compared this approximate method with an exact  $\chi^2$  calculation and found that the error is only about  $\pm 3\%$ . The results for the  $\chi^2/\text{datum}$  are shown in Table I and Fig. 2. To get an idea for the dependence of our results on the SFR parameter  $\tilde{\Lambda}$ , we conduct one series of  $\Lambda$  variations with  $\tilde{\Lambda}$  fixed at 700 MeV and another one for  $\tilde{\Lambda} \rightarrow \infty$ , which is equivalent to dimensional regularization (DR). As mentioned, NLO does not really need SFR, which is why we include the case of DR. As can be clearly seen from Table I, the dependence on  $\tilde{\Lambda}$  is very weak, which is comforting.

For the energy interval 2-35 MeV, the reproduction of the  $np$  data is very good for all cutoffs in the range

TABLE II: Same as Table I, but for NNLO. The two choices for the SFR parameter are  $\tilde{\Lambda} = 700$  MeV and  $\tilde{\Lambda} = 600$  MeV (in parentheses).

$T_{\text{lab}}$ bin (MeV)	$\Lambda$ (MeV)							
	400	450	500	600	700	800	850	900
2–35	0.91 (0.91)	0.88 (0.90)	0.87 (0.89)	0.87 (0.88)	0.87 (0.88)	0.87 (0.87)	0.87 (0.87)	0.98 (0.99)
35–125	6.36 (9.50)	2.80 (4.53)	1.96 (2.92)	1.88 (2.19)	2.27 (2.21)	2.24 (2.23)	2.23 (2.26)	2.21 (2.30)
125–183	52.2 (78.1)	15.0 (31.0)	6.40 (19.5)	4.33 (16.6)	6.22 (17.2)	8.75 (18.3)	9.73 (18.7)	16.4 (18.7)
183–290	149 (194)	40.9 (76.2)	18.9 (52.1)	18.0 (54.8)	23.1 (56.1)	27.8 (54.4)	28.2 (52.0)	50.2 (48.4)

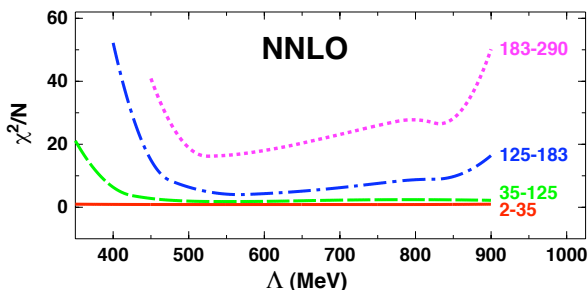


FIG. 3: (color online). Same as Fig. 2, but for NNLO.

$\Lambda = 350 - 800$  MeV where  $\chi^2/\text{datum} \lesssim 2$  is obtained. However, this should not come as a surprise since the  $S$ -waves are fit around zero energy and the  $P$ -waves at 25 MeV. Thus, the results for the 2-35 MeV interval are not predictions. The first predictions of the theory appear at the interval 35-125 MeV. For  $\Lambda$  between 500 to 850 MeV, the  $\chi^2/\text{datum}$  stays around  $5 \pm 1$  which may be perceived as moderate cutoff independence. Note that a  $\chi^2/\text{datum}$  around 5 signifies a good qualitative reproduction of the data. Finally, in the third energy interval shown in Table I, namely, 125-183 MeV, the  $\chi^2/\text{datum}$  is 70 or larger, which simply means that the data are not reproduced. Under these circumstances a discussion of  $\Lambda$  independence is out of place.

In summary, chiral EFT at NLO is able to describe  $NN$  scattering up to about 100 MeV laboratory energy with moderate regulator independence for  $\Lambda$ 's between 500 and 850 MeV.

## B. Renormalization at NNLO

At NNLO, we use  $n = 3$  in the regulator function Eq. (3) and calculate the  $\chi^2$  exactly by applying Eq. (58) explicitly to the 1999 data base [34], which includes 559

$np$  data for the interval 2-35 MeV, 579  $np$  data for 35-125 MeV, 414  $np$  data for 125-183 MeV, and 846  $np$  data for 183-290 MeV. The results of these  $\chi^2/\text{datum}$  calculations are shown in Table II. We also check the dependence of our results on the SFR parameter  $\tilde{\Lambda}$ , for which we apply two choices, namely, 700 MeV and 600 MeV. The results for  $\tilde{\Lambda} = 600$  MeV are given in parentheses. The dependence on  $\tilde{\Lambda}$  is moderate up to 125 MeV. However, significant differences occur above 125 MeV with the choice  $\tilde{\Lambda} = 600$  MeV producing larger  $\chi^2$ . This may be seen as an indication that  $\tilde{\Lambda} = 600$  MeV cuts out too much from the 2PE contribution. We have also checked  $\tilde{\Lambda} = 800$  MeV, but found that spurious bound states and resonances start to occur, which SFR is supposed to prevent. Thus,  $\tilde{\Lambda} = 700$  MeV appears to be the optimal choice at NNLO. This is not unreasonable on general grounds. If the 2PE is described in terms of  $2\pi$  resonances, we have the  $\sigma(600)$  with a mass of 400-1200 MeV and the  $\rho(770)$  with mass 775 MeV and width 150 MeV [35]. The choice  $\tilde{\Lambda} = 600$  MeV cuts out the contributions from all mass components  $\geq 600$  MeV, which obviously will trim the  $\sigma$ - and  $\rho$ -like contributions severely. On the other hand,  $\tilde{\Lambda} = 700$  MeV will keep substantial contributions from  $\sigma$  and  $\rho$  alive.

The  $\chi^2$  as a function of  $\Lambda$  with  $\tilde{\Lambda}$  fixed at 700 MeV are plotted in Fig. 3. The curves in this figure clearly reveal that, for all energy intervals above 35 MeV, a cutoff  $\Lambda \lesssim 450$  MeV cuts out too much from the intermediate range part of the  $NN$  potential, such that, particularly, the higher energies are not described well (large  $\chi^2$ ). Then, on the other other end of the  $\Lambda$  spectrum, the  $\chi^2$  rise again for  $\Lambda \gtrsim 850$  MeV, when too much of the unknown short-distance dynamics is admitted. In between the two extremes, namely for  $450 \text{ MeV} \lesssim \Lambda \lesssim 850 \text{ MeV}$ , one can clearly identify plateaus for all energy intervals. This demonstrates cutoff independence for the physically relevant range and, thus, successful renormalization.

At NNLO, the reproduction of the  $NN$  data is acceptable up to about 200 MeV laboratory energy, which is about 100 MeV above the limitations of the theory at



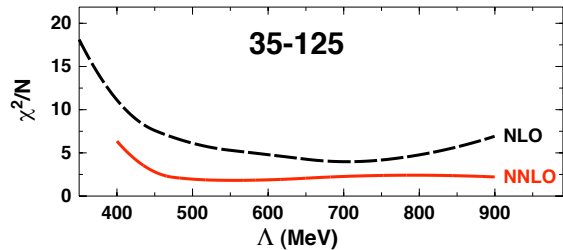


FIG. 4: (color online).  $\chi^2/\text{datum}$  for the reproduction of the  $np$  data in the energy range 35-125 MeV as a function of the cutoff parameter  $\Lambda$  of the regulator function Eq. (3). The (black) dashed curve shows the  $\chi^2/\text{datum}$  achieved with a potential constructed at order NLO and the (red) solid curve is for NNLO. The SFR parameter is always  $\tilde{\Lambda} = 700$  MeV.

NLO.

### C. Order by order improvement

Besides regulator independence, a proper EFT should also show order-by-order improvement of the predictions with decreasing error. We address this issue in Fig. 4 for the energy interval 35-125 MeV and in Fig. 5 for 125-183 MeV. In each figure, we show the NLO and NNLO  $\chi^2$  results for easy comparison. The figures clearly demonstrate that, when going from NLO to NNLO, the  $\chi^2$  is drastically reduced and, at the same time, the  $\Lambda$ -independence substantially improved. This is exactly what one wants to see in an EFT.

It is important to stress that NLO and NNLO have the same number of contact parameters. Thus, the improvements seen at NNLO are not due to a larger number of fit parameters. The difference at NNLO is an improved 2PE contribution to the  $NN$  interaction. At this order, the subleading  $\pi\pi NN$  vertices from the dimension-two Lagrangian with LECs  $c_i$  contribute [cf. Eqs. (33)-(36)]. These vertices represent correlated 2PE as well as intermediate  $\Delta(1232)$ -isobar excitation. It is well-known from the conventional meson theory of nuclear forces [13] that these two mechanisms are crucial for a realistic and quantitative 2PE model. Consequently, at NNLO, the chiral 2PE assumes a realistic size and describes the intermediate-range attraction of the nuclear force right. This explains the improvements seen at NNLO, which are

demonstrated in a particularly impressive way in Fig. 5.

## IV. CONCLUSIONS

We have investigated the nonperturbative renormalization of nucleon-nucleon scattering at next-to-leading order (NLO) and next-to-next-to-leading order (NNLO)

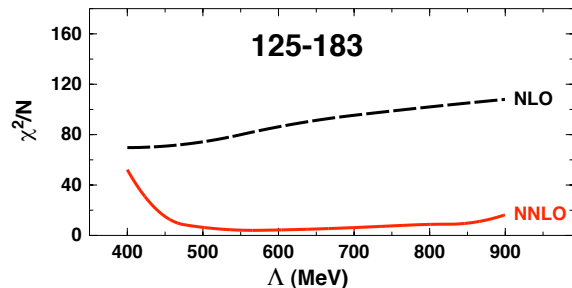


FIG. 5: (color online). Same as Fig. 4, but for the energy range 125-183 MeV.

of chiral effective field theory. We keep the cutoff parameter  $\Lambda$  below the chiral symmetry breaking scale of about 1 GeV. The accuracy of the fits is measured by the  $\chi^2$  for the reproduction of the  $NN$  data. Applying this measure, we find that, at NLO, the  $NN$  data are described well up to about 100 MeV laboratory energy and, at NNLO, up to about 200 MeV. Concerning the cutoff dependence, we can clearly identify plateaus of insensitivity to changes of  $\Lambda$  for  $450 \text{ MeV} \lesssim \Lambda \lesssim 850 \text{ MeV}$ . We perceive this result as successful renormalization of the chiral  $NN$  interaction at the two orders considered in this study.

### Acknowledgements

This work was supported in part by the U.S. Department of Energy under Grant No. DE-FG02-03ER41270. The work of D. R. E. was funded by the Ministerio de Ciencia y Tecnología under Contract No. FPA2010-21750-C02-02 and the European Community-Research Infrastructure Integrating Activity “Study of Strongly Interacting Matter” (HadronPhysics3 Grant No. 283286).

- 
- [1] R. Machleidt and D. R. Entem, Phys. Rep. **503**, 1 (2011).  
 [2] E. Epelbaum, H.-W. Hammer, and U.-G. Meißner, Rev. Mod. Phys. **81**, 1773 (2009).  
 [3] J. Gasser and H. Leutwyler, Ann. Phys. (N.Y.) **158**, 142 (1984).  
 [4] J. Gasser, M. E. Sainio, and A. Švarc, Nucl. Phys. **B307**,

- 779 (1988).  
 [5] S. Weinberg, Phys. Lett **B251**, 288 (1990); Nucl. Phys. **B363**, 3 (1991).  
 [6] C. Ordóñez, L. Ray, and U. van Kolck, Phys. Rev. Lett. **72**, 1982 (1994); Phys. Rev. C **53**, 2086 (1996).  
 [7] N. Kaiser, R. Brockmann, and W. Weise, Nucl. Phys.

- A625**, 758 (1997).
- [8] E. Epelbaum, W. Glöckle, and U.-G. Meißner, Nucl. Phys. **A637**, 107 (1998).
- [9] E. Epelbaum, W. Glöckle, and U.-G. Meißner, Nucl. Phys. **A671**, 295 (2000).
- [10] D. R. Entem and R. Machleidt, Phys. Rev. C **66**, 014002 (2002).
- [11] D. R. Entem and R. Machleidt, Phys. Rev. C **68**, 041001 (2003).
- [12] E. Epelbaum, W. Glöckle, and U.-G. Meißner, Nucl. Phys. **A747**, 362 (2005).
- [13] R. Machleidt, K. Holinde, and Ch. Elster, Phys. Rep. **149** (1987) 1.
- [14] S. Weinberg, *Effective Field Theory, Past and Future*, arXiv:0908.1964 [hep-th].
- [15] D. B. Kaplan, M. J. Savage, and M. B. Wise, Nucl. Phys. **B478**, 629 (1996).
- [16] A. Nogga, R. G. E. Timmermans, and U. van Kolck, Phys. Rev. C **72**, 054006 (2005).
- [17] C.-J. Yang, Ch. Elster, D. R. Phillips, Phys. Rev. C **80**, 044002 (2009).
- [18] M. Pavon Valderrama, and E. Ruiz Arriola, Phys. Rev. C **74**, 064004 (2006).
- [19] D. R. Entem, E. Ruiz Arriola, M. Pavón Valderrama, and R. Machleidt, Phys. Rev. C **77**, 044006 (2008)
- [20] Ch. Zeoli, R. Machleidt, D. R. Entem, Few-Body Syst. DOI 10.1007/s00601-012-0481-4, arXiv:1208.2657 [nucl-th].
- [21] E. Epelbaum and J. Gegelia, Eur. Phys. J. **A41**, 341 (2009).
- [22] E. Epelbaum and J. Gegelia, Phys. Lett B **716**, 338 (2012).
- [23] B. Long, and U. van Kolck, Ann. Phys. (N.Y) **323**, 1304 (2008)
- [24] M. P. Valderrama, Phys. Rev. C **84**, 064002 (2011)
- [25] R. Machleidt, P. Liu, D. R. Entem, and E. R. Arriola, Phys. Rev. C **81**, 024001 (2010)
- [26] G. P. Lepage, *How to Renormalize the Schrödinger Equation*, arXiv:nucl-th/9706029.
- [27] E. Epelbaum, W. Glöckle, and U.-G. Meißner, Eur. Phys. J. **A19**, 401 (2004).
- [28] P. Büttiker and U.-G. Meißner, Nucl. Phys. **A668**, 97 (2000).
- [29] R. Blankenbecler and R. Sugar, Phys. Rev. **142**, 1051 (1966).
- [30] E. Epelbaum and U.-G. Meißner, *On the renormalization of the one-pion exchange potential and the consistency of Weinberg's power counting*, arXiv:nucl-th/0609037.
- [31] V. G. J. Stoks, R. A. M. Klomp, M. C. M. Rentmeester, and J. J. de Swart, Phys. Rev. C **48**, 792 (1993).
- [32] R. A. Arndt, I. I. Strakovsky, and R. L. Workman, SAID, Scattering Analysis Interactive Dial-in computer facility, George Washington University (formerly Virginia Polytechnic Institute), solution SM99 (Summer 1999); for more information see, e. g., R. A. Arndt, I. I. Strakovsky, and R. L. Workman, Phys. Rev. C **50**, 2731 (1994).
- [33] V. Stoks and J. J. de Swart, Phys. Rev. C **47**, 761 (1993); and V. Stoks, private communication.
- [34] The 1999 data base is defined in: R. Machleidt, Phys. Rev. C **63** 024001 (2001).
- [35] K. Nakamura *et al.*, J. Phys. G: Nucl. Part. Phys. **37**, 075021 (2010).